Chuvieco, E. et al. (2020) 'Satellite Remote Sensing Contributions to Wildland Fire Science and Management', Current forestry reports, 6(2), pp. 81–96.

Available at http://dx.doi.org/10.1007/s40725-020-00116-5

Satellite Remote Sensing Contributions to Wildland Fire Science and Management

Emilio Chuvieco[1] · Inmaculada Aguado[1] · Javier Salas[1] · Mariano García[1] · Marta Yebra[2,3,4] · Patricia Oliva[5]

Abstract

Purpose This paper reviews the most recent literature related to the use of remote sensing (RS) data in wildland fire management. **Recent Findings** Studies dealing with pre-fire assessment, active fire detection, and fire effect monitoring are reviewed in this paper. The analysis follows the different fire management categories: fire prevention, detection, and post-fire assessment. Extracting the main trends from each of these temporal sections, recent RS literature shows growing support of the combined use of different sensors, particularly optical and radar data and lidar and optical passive images. Dedicated fire sensors have been developed in the last years, but still, most fire products are derived from sensors that were designed for other purposes. Therefore, the needs of fire managers are not always met, both in terms of spatial and temporal scales, favouring global over local scales because of the spatial resolution of existing sensors. Lidar use on fuel types and post-fire regeneration is more local, and mostly not operational, but future satellite lidar systems may help to obtain operational products. Regional and global scales are also combined in the last years, emphasizing the needs of using upscaling and merging methods to reduce uncertainties of global products. Validation is indicated as a critical phase of any new RS-based product. It should be based on the independent reference information acquired from statistically derived samples.

Summary The main challenges of using RS for fire management rely on the need to improve the integration of sensors and methods to meet user requirements, uncertainty characterization of products, and greater efforts on statistical validation approaches.

Keywords Fire · Wildland · Remote sensing · Satellite earth observation · Validation · Lidar · Landsat · MODIS · Sentinel · VIIRS

✉ Emilio Chuvieco
emilio.chuvieco@uah.es

Inmaculada Aguado
inmaculada.aguado@uah.es

Javier Salas
javier.salas@uah.es

Mariano García
mariano.garcia@uah.es

Marta Yebra
marta.yebra@anu.edu.au

Patricia Oliva
patricia.oliva@umayor.cl

[1] Environmental Remote Sensing Research Group, Department of Geology, Geography and the Environment, Universidad de Alcalá, Calle Colegios 2, 28801 Alcalá de Henares, Spain

[2] Fenner School of Environment & Society, Australian National University, Canberra, Australia

[3] Research School of Aerospace, Mechanical & Environmental Engineering, Australian National University, Canberra, Australia

[4] Bushfire and Natural Hazards Cooperative Research Center, Melbourne, Australia

[5] Hémera Centro de Observación de la Tierra, Escuela de Ingeniería Forestal, Facultad de Ciencias, Universidad Mayor, Santiago, Chile

Introduction: Why Using RS Methods in Fire Management?

Remote sensing sensors offer global information, at different spatial resolutions and different spectral regions. They observe systematically the Earth surface, therefore providing ideal conditions for multitemporal analysis. In addition, they derive information without destructive sampling. All these properties explain the wide use of RS data in fire-related research and management since the early 1970s. The first applications were based on visual analysis of aerial photography. After the launch of the Landsat satellite in 1972, satellite data have been used for the different phases of fire management: before the fire, to estimate fire danger conditions; during the fire, to detect active fires and estimate fire behaviour, and after the fire, to analyse fire effects and vegetation recovery [1].

Nowadays, contributions of remote sensing methods to wildland fire science comprise a wide range of sensors, including ground spectroradiometers, cameras mounted on helicopters, airplanes and unmanned aerial vehicles, and satellite missions, some of which are specifically designed to target fire activity or include specific bands for this objective. The range of interpretation methods has also greatly expanded in the last decades, including machine learning algorithms [2•, 3]; synergy between optical and thermal data [4], between optical and radar [5], or between optical passive and lidar [6]; the extended use of radiative transfer models [7]; and more elaborate change detection analysis [8].

We review in this paper the main research trends on the use of satellite RS methods for fire science and management, particularly those published in the last 5 years (> 2014). Our analysis was based on a Web of Science quest conducted in September 2019. We searched for papers including "fire" and "remote sensing" or "fire" and "satellite" in the title or abstract. This search contained all sources referenced in the Science Citation Index (SCI), Social Sciences Citation Index (SSCI), and Arts & Humanities Citation Index (A&HCI). The total number of references found was 4808, starting in 1972 and ending in August 2019, with a clear increasing trend (Fig. 1). Most of these references were journal papers (96%), with very minor representation of proceedings. These manuscripts were classified in the environmental sciences (30%), including meteorology and atmosphere (27%), ecology (11%), forestry (10%), physical geography (6%), biodiversity (3%), and water resources (2.5%) (Please note that these categories may overlap). Remote Sensing was also a very important class, assigned to 23% of all citations. The most active journals for the whole time series were the Journal of Geophysical Research Atmospheres, Remote Sensing of Environment, Atmospheric Chemistry and Physics, International Journal of Remote Sensing, International Journal of Wildland Fire, Remote Sensing, Atmospheric Environment, Geophysical Research Letters and Forest Ecology and Management, which accounted for 40% of all references.

We have selected for this review the 1924 papers published in the last quinquennial. The sources are similar to the complete list of journals, although over the last years, the most active was *Remote Sensing*, followed by *Atmospheric Chemistry and Physics*, *Remote Sensing of Environment*, and the *International Journal of Wildland Fire*. As the selected references included many similar studies, either in terms of methods or study regions, we have only quoted those that, according to the authors' judgement, provide more novelty to the field. We have organized the review around the three main temporal phases of fire management, including fire danger assessment (mainly focused on determining fuel conditions), fire detection (location and monitoring of active fires), and fire effects assessment (including post-fire changes and vegetation recovery after a fire).

RS in Fire Danger Assessment

Fire danger is a combination of a wide variety of topics, from which weather, fuel, and human factors are the most relevant. In this topic, RS has contributed mostly to the characterization of fuel state and conditions, including moisture content (FMC), biomass, canopy cover, and horizontal-vertical continuity.

Better estimation of spatial and temporal variations of fire danger conditions is critical for fire prevention. In this respect, the contributions of RS to fire management are particularly relevant. For instance, quantifying when and where vegetation is dry enough to facilitate fire ignition or propagation is vitally important for strategic planning. Additionally, this information is useful to locate containment lines (e.g. fuel moisture content variations can be used as soft containment lines) and help with the firefighting strategies (e.g. lidar-derived fuel load maps to locate sites free of trees to winch specialist firefighters in or to try to pick the easiest line to construct walking tracks to the fire). This information can equally be used as part of preseason planning when fire agencies and land management departments formulate their seasonal outlook for fire and map at-risk areas as well as for planning and undertaking prescribed burns. Fire managers need to know the moisture content of the planned burn area to know whether it is going to be successful because if it is too wet, it will not burn, but if it is too dry, it can be over-burned or escape.

Fuel Moisture Content

Fuel moisture content (FMC) is the ratio of the mass of water contained in a plant to its total dry mass. Research has shown that there are clear thresholds of FMC (in both dead and live fuels) associated with the occurrence of wildfires [9–11], and

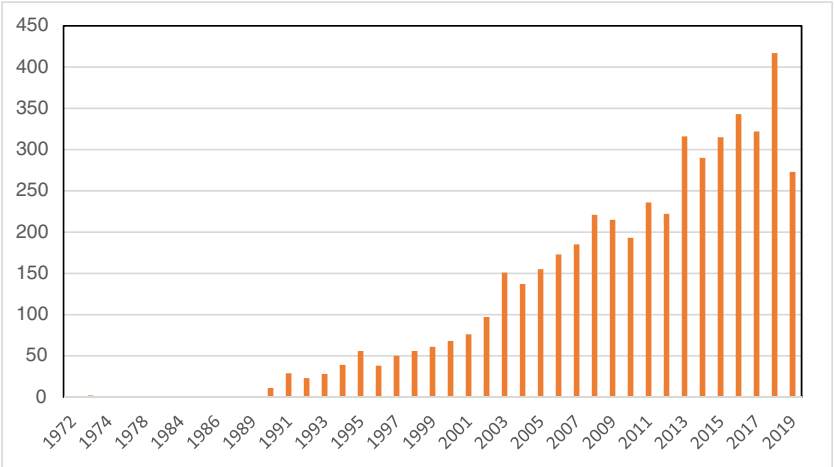

Fig. 1 RS&Wildfire papers published since 1972 in the WoS. Note that 2019 only covers January to August

therefore quantifying when and where forests are approaching critical dryness levels is vitally important for assessing wildfire risk and for planning management burns. Since this temporal dimension is critical for operational use of FMC estimations, most satellite products have relied on high-temporal resolution (though low spatial resolution) sensors, such as MODIS, AVHRR and, VEGETATION. Recent developments based on medium spatial resolution images (Landsat or Sentinel-1&2) are still very scarce.

FMC can be retrieved using optical remote sensing data given the effect that water has on the spectra reflectance through absorption of radiation within the near infrared (NIR) and short-wave infrared (SWIR) spectral regions [7]. Most prior work that has used remote sensing data to estimate FMC has been carried out in Mediterranean ecosystems in Europe and western North America [7]. These studies demonstrate that radiative transfer modelling approaches, which are based on relationships between leaf chemical and optical properties, are more robust than traditional empirical approaches and more easily to generalize as they are not site dependent. Recently, Yebra et al. [12•] showed that a radiative transfer modelling approach developed in Europe had similar accuracy to statistical models when applied to Australian ecosystems using the same sensor (Moderate Resolution Imaging Spectroradiometer, MODIS). However, the reported accuracy in some forests, such as the eucalypt forest, was still not high enough for fire management operations, given that these species have different radiative transfer properties to European species [12•].

Microwave data has also been found to be sensitive to FMC, given that changes in dielectric constant associated with moisture impact the radar backscatter measurements [13]. The use of microwave images for retrieval of FMC is more complex than with optical sensors and presents different factors of potential confusion, such as vegetation biomass, height, topographic position, or roughness, and, therefore, it has not been explored as much as optical data. Recently, Wang et al. [14] demonstrated the capability of C-band Sentinel-1A data for forest FMC retrieval by coupling the bare soil backscatter linear model with the vegetation backscatter water cloud model. Jia et al. [15] presented a new multivariant regression model to estimate FMC in the Mediterranean ecosystem of Southern California, using the Soil Moisture Active Passive (SMAP) L-band radiometer estimations of soil moisture conditions.

Despite advances in near-real-time modelling of FMC using satellite data, there are risk assessment operational needs that current methods cannot fill in. For example, remote sensing approaches cannot provide the stand-level detail required for operational fire management, such as differences in FMC between shrubs and trees, or the forecasting of moisture values. Drought indices can be used to forecast FMC but do not provide reliable predictions [16]. The development of a physiologically based FMC model may improve those forecasts, which are critically important for operational planning [17]. However, there has been little research on the ecophysiological drivers of FMC. Recently, Nolan et al. [18] investigated the relationships between FMC and plant physiological traits (including leaf water potential, stomatal conductance, and cellular osmotic and elastic adjustments) in Mediterranean tree and shrub species and demonstrated that incorporating plant physiological traits can significantly improve process-based predictions of FMC. They found that midday moisture, which generally represents minimum daily values, could be reliably modelled from predawn leaf water potential (Ψleaf) and that such a model outperformed commonly applied drought indices. Consequently, a way forward to forecast FMC should combine recent advances in the remote sensing and physiological understanding of FMC into one integrated approach.

Regardless of the method used to retrieve FMC, validation of FMC estimations is quite challenging, as it requires continuous field measurements. To help the generation of global FMC products, Yebra et al. [19] recently compiled an

extensive global database of live fuel moisture content (LFMC) measurements. The database contains 161,717 individual records based on in situ destructive samples that have been generated from different projects worldwide. These measurements have been typically used to calibrate and validate remote sensing FMC estimation algorithms.

Fuel Types

Fuel types represent vegetation classes that have similar fire behaviour [20]. In order to introduce fuel characteristics into fire behaviour and fire effect simulation models, fuel types are parameterized using fuel models [21], which organize fuels into groups according to the main fire propagation media. Different classification schemes have been proposed for different regions [22, 23]. The most recent trends related to fuel type mapping from RS methods take advantage of different hybrid approaches, which mostly merge lidar and passive optical data. Critical properties of fuels such as amount, size, or arrangement can be accurately estimated from lidar, while information on the main fire carrier, i.e. vegetation type, can be obtained from multispectral data.

Explicit information on fuel properties and their spatial distribution is critical for improving our understanding of fire behaviour and effects. Because these properties represent structural rather than functional characteristics of the forest fuels, most fuel type studies nowadays use lidar data. This technique is based on estimating heights from very accurate measurements of time intervals between sending and receiving a laser pulse. Ground and airborne lidar systems are the most common nowadays, although the ICESat-1 mission provided accurate estimations of fuel properties [24]. Over the next few years, satellite lidar observations will greatly increase with the recent launch of ICESat-2 and the Global Ecosystem Dynamics Investigation (GEDI) missions. The canopy variables estimated from lidar have included fuel load (CFL), canopy height (CH) [25], canopy base height (CBH), canopy bulk density (CBD), and fractional cover (CC), which are particularly important for crown fire propagation. The statistical modelling approach generally used is multivariate linear regression given its simplicity and good performance. More recently, a few studies have used machine learning techniques for modelling canopy fuel properties from lidar data, such as random forest [26] or support vector machines [27]. CH and CC are well estimated by lidar measurements. However, CBH and CBD, which require a description of the vertical distribution of canopy fuels, showed lower accuracies. Factors affecting the accuracy of the estimation of these canopy variables include the point density of the lidar datasets and the structural characteristics, for instance, canopy permeability of the analysed stand [26, 28]. Romero Ramirez et al., [29] did not find significant differences between estimates of CFL derived using 2 points/m^2 or lower, suggesting that improving the accuracy of the estimates requires higher point densities similar to those provided by terrestrial lidar [30].

The 3D information provided by lidar sensors allows for a complete vertical characterization of the fuel distribution including surface fuel properties [31]; nevertheless, the accuracies of the estimated variables are lower than those of the upper canopy. This is due to the attenuation of the signal that results in the undersampling of the lower vegetation layers [32]. Bright et al. [26] estimated surface fuel properties including litter and duff, 1 to 100-h, 1000-h, and total surface fuels with R^2 values ranging between 16 and 30% and RMSE values varying between 39 and 99%.

The simplest approach to integrating passive and active sensors relies on merging both into a single dataset that is subsequently used to run a classification algorithm. Given the high dimensionality of the resulting dataset, principal component analysis (PCA) or minimum noise fraction (MNF) techniques have been applied to extract the most significant variables [33]. Other approaches to data integration have used a two-step method. In the first phase, the main vegetation types are mapped using optical passive sensors, while in the second one, fuel types are discriminated using decision rules applied to lidar-based information. This approach, originally applied by García et al. [34•], was extended by Marino et al., [35] to two different fuel classification systems. The good results obtained for both showed the robustness of the approach. Stavros et al. [36] used a similar methodology: a dominant vegetation type and structural information were derived from AVIRIS and lidar data, respectively. Likewise, Sanchez et al. [37] mapped vegetation types from Sentinel-2 data and characterized vegetation structure from low-density airborne lidar data. The integration of the fuel type maps, with climatic and topographic data, allowed the authors to compute ignition probability.

Contrary to mapping fuel types, the fusion of lidar and optical data to estimate the above-mentioned properties of surface and canopy fuels did not result in a significant improvement due to the much-limited sensitivity of passive optical data to structure as compared with lidar. However, the integration of lidar and satellite data offers possibilities to overcome the restrictions of the limited spatial and temporal coverage of airborne lidar data. Thus, methods have been developed to extrapolate lidar-based fuel properties. For instance, Garcia et al. [27] developed a two-step approach to extend accurate local lidar estimates to larger regions based on Landsat data using a machine learning approach, obtaining R^2 values of 0.8, 0.79, and 0.64 and RMSE of 3.76 Mg ha^{-1}, 0.09, and 0.02 kg m^{-3} for CFL, CC, and CBD, respectively. Likewise, optical and SAR data were integrated in order to extrapolate lidar CH regionally over different biomes [38].

The main limitation of lidar data is the cost of flight campaigns and restriction to local scales, although some countries (Spain, Slovenia, Stonia, Denmark) have already undertaken

wall-to-wall lidar inventories that help the generalized use of these data to update and parameterize existing fuel type maps. Temporal coverage is another constraint of airborne lidar campaigns. Because of current limitations of lidar data for operational fuel type mapping, many studies still rely only on passive optical data. For instance, Stefanidou et al. [39] compared the operational capabilities of Landsat OLI data and Disaster Monitoring Constellation (DMC) data applying an object-based classification methodology to classify fuel types. Bajocco et al. [40] proposed a different concept of fuel types defining phenological fuel classes. This concept attempts to characterize fuels based on functional properties such as productivity and seasonality, related to fuel accumulation and flammability respectively, rather than the structural ones.

Another trend in fuel mapping is the use of an OBIA (object-based image analysis) approach. This approach provides a more homogeneous representation of fuel types than pixel-based methods, allowing for the identification of complex objects, which are common for fuel type characterization [33].

Detection of Active Fires

Active fires (AF) have been detected by middle- and thermal-infrared observations since the 1980s using mostly polar-orbiting meteorological satellites [41]. The physical basis of AF detection relies on the high thermal contrast between hotspots and the background in the middle-infrared region (3–5 μm). This channel was included in the first meteorological missions (such as the NOAA-AVHRR sensor) for cloud detection. Even though these sensors have low thermal sensitivity, they provided the first global analysis of fire activity [42]. Later on, the development of dedicated AF sensors greatly improved the quality of these products, particularly after the launch of MODIS, on board the Terra and Aqua satellites. Over the last few years, the use of active fire (AF) datasets for research and operational applications has expanded to geostationary (Meteosat, GOES, Himawari) and medium-resolution satellites (such as Landsat-8 or Sentinel-2) and even to unmanned aerial vehicles for specific areas. Satellite detections of active fires are particularly relevant during a fire crisis, to obtain a first assessment of anomalous conditions in the case of extreme fire seasons. Recent exceptional fires within South America (2019: [43]) and Australia (2020), for instance, have been extensively shown in the media through satellite active fire products, most commonly obtained from MODIS or VIIRS detections. During these crises, AF products derived from different satellite systems have been extensively used to support fire management systems, introduced as input in numerous air quality [44, 45] and carbon emission estimation methodologies [46–48]. They have also been used for fire behaviour models [49], to estimate fire spread rate [50] and to detect gas flares [51] and volcanic activity [52].

The new generation of geostationary satellites provides observations every 10 to 15 min at an improved spatial resolution (2–3 km) making it possible to detect short-lived fires not detectable by polar-orbiting satellites and to track in detail the evolution of the fire line and fire radiative power [53]. In addition, they have enhanced sensors that provide information on 12–16 spectral bands with improved radiometry of 10–14 bits (Table 1). They introduce a substantial improvement in spatial, temporal, spectral, and radiometric resolution over their predecessors, which correspondingly relates to an enhanced capability for fire detection [54].

Several authors developed new algorithms aiming to improve the active fire detection products available [55]. MSG-SEVIRI and GOES-ABI sensors offer operational AF products, which are built on the heritage of the algorithms developed for previous sensors [53]. As Himawari-AHI is not producing an operational AF product yet, several algorithms have been developed for active fire detection using these data [54, 56]. Recent papers try to apply the same geostationary AF detection algorithms to different satellites, for instance, Himawari-8 and MSG-SEVIRI, with the objective of producing a harmonized product of AF detections from geostationary sensors [55]. However, other authors pointed out the importance of adapting the algorithms to the sensor characteristics, as it was shown that better estimations were obtained from MSG-SEVIRI than for GOES-ABI AF detections, even when the former has lower spatial resolution [54].

While an advantage of geostationary sensors is their temporal resolution, the polar-orbiting sensors have finer spatial resolution, which ensures higher accuracy at locating and mapping thermal anomalies. AF detections are produced using different polar-orbiting sensors, such as MODIS [57•], the Visible Infrared Imaging Radiometer Suite (VIIRS) [58, 59], FengYun-3C VIRR [60], Landsat-8 OLI [61], TET-1 [62], and FireBird [63].

Currently, the best compromise between spatial and temporal resolution is provided by the operational active fire product derived from the 375 m VIIRS bands on board the National Polar-Orbiting Partnership (NPP) satellite since 2013 and on board the NOAA-20 since 2017 [64]. Its improved resolution, frequent acquisitions, and higher sensitivity to burning pixels allow the direct estimation of the burned area by aggregation of consecutive fire detections [58] and the estimation of fire-driven deforestation [65]. With two satellites in operation, the 375 m AF product time lapse between acquisitions is reduced to a few hours ensuring a higher frequency of observations providing fire behaviour to fire managers and atmospheric modellers with higher resolution active fire data. Besides, VIIRS Day/Night band has also been used to develop an AF detection algorithm that exploits visible-light and infrared spectral response of AF at night [66]. This night-time

Table 1 Main sensors currently used for active fire detection

Sensor	MSG-11 SEVIRI	Advanced Himawari Imager-8	GOES-16 ABI	GOES-17 ABI	Terra & Aqua MODIS	NPP & NOOA-20-VIIRS
Spatial resolution	3 km	2 km	2 km	2 km	250–500–1000 m	375–750 m
Spectral bands	12	16	16	16	2–5–29	5–16
Temporal resolution*	5–15 min	10 min	5–15 min	5–15 min	12 h	12 h
Radiometric resolution (bits)	10	14	14	14	10	10
Launched on	2015	2014	2016	2018	2002	2012
Operational full disk	Feb-2018	July 2015	Dec-2018	Feb-2019		
Satellite type	Geostationary	Geostationary	Geostationary	Geostationary	Polar-orbiting	Polar-orbiting
Centred at	0°	140.7°	75.2°	137.2°		
Operational fire product (spatial resolution)	Yes (3 km)	No	Yes (2 km)	No	Yes (1000 m)	Yes (375 m)

The number of bands in the Polar-orbiting sensors matches the range of spatial resolution of each sensor. *Temporal resolution of geostationary sensors refers to the nominal resolution of a full disk image acquisition

algorithm improves the number of detected AF pixels in large fires (up to 90%) in comparison with the VIIRS 750 m AF product [59].

Most of the algorithms developed in the last few years are mainly based on the use of contextual tests to detect thermal anomalies that rely on the determination of the background temperature and the analysis of the strong contrast in brightness temperature between the potential fire pixel and the low background temperature [53, 57•, 64]. The pixel is classified as a potential fire pixel when the contrast is higher than a specified threshold [57•]. The dependence on the background temperature is the main reason why these algorithms produce high omission of small fires, since an error of 1 K in the background brightness temperature may result in the masking of small fires because the contrast is not high enough to classify them as potential fire pixels. The algorithms developed on a global scale are designed in a conservative way to avoid false alarms, which may produce a high percentage of AF omission in areas where fires have a lower brightness temperature. In order to improve the AF detection, several authors developed regional algorithms focused on detecting the low-intensity thermal anomalies occurring in those regions, such as Alaska [67] or China [68]. On the other hand, novel AF algorithms include also the temporal dimension in their classification process [60, 61]. The temporal dimension of these algorithms allows separation between permanent heat sources and new fire events, facilitating earlier detection of the fires and the removal of false alarms derived from bright surfaces.

Common bands used in AF detection algorithms are the medium-infrared bands, located around 3–4 μm, and the thermal infrared bands, centred at 10–11 μm [53, 57•]. The different spectral behaviour of active fire pixels in both bands is the main characteristic leading the algorithm procedure. Recent algorithms, aiming to detect AF from Landsat observations, are based on spectral changes in the NIR and SWIR spectral regions [61, 69].

The role of the smouldering phase of the fire is increasingly taking more attention from researchers, especially in peatland fires where most of the emissions released to the atmosphere are produced by smouldering combustion [70•, 71]. Consequently, several papers have studied the identification of different phases of fire combustion to improve the estimation of gases emitted in the burning process [72, 73] or just to improve the detection of peat fires [63].

RS of Fire Effects

One of the most obvious applications of satellite observations to wildland fire science and management is the estimation of fire impacts, most commonly by assessing burned area (BA). There are still only a few countries that have reliable wildfire statistics. Therefore, global fire occurrence based on national estimations is likely to be very inaccurate. Satellite earth observation is the most practical way of estimating BA at global scales. Since active fires are only a temporal sample of actual burning activity (at the satellite overpass), the most adequate method to estimate BA is the analysis of reflectance or thermal changes caused by the fire. Existing products include several spatial scales, ranging from local to national and global datasets. Obviously, the latter will be produced at lower spatial resolution and from coarse resolution sensors. More detailed products are routinely generated only for some regions, based on Landsat or Sentinel-2 data, but still much effort is required to use them operationally for generating fire statistics.

Several global BA products have been released in the last years, mainly derived from sensors providing frequent temporal coverage (daily), such as MODIS, MERIS, or VEGETATION, but poor spatial detail (> 300 m). A recent review by Chuvieco et al. [74••] shows the strengths and limitations of existing global products. The most reliable ones estimate total worldwide BA in the range of 3.5 to

4.5 Mkm^2 [74••], but this estimation is likely to be conservative since comparison of global and regional products shows an important underestimation from the former [75•, 76]. Now the most used global BA product is the MCD64A1, produced by NASA based on MODIS 500-m reflectance bands guided by active fires. The last version is collection 6 [77•], which has superseded other NASA BA products. The ESA's Climate Change Initiative Fire Disturbance project (FireCCI) has recently developed an alternative global BA product, based on MODIS 250 m reflectance bands, which provides similar accuracy to the NASA product but seems more sensitive to small burn patches [78, 79•]. A prototype for generating BA products from long-term series of AVHRR data has also been recently published [80].

These global BA products have been extensively used for the analysis of fire activity, determining characteristics of fire regimes, such as average BA and temporal persistency [81], and spatial variations of BA trends [82•]. These trends are then related to the main drivers of fire, including climate changes and human activity [83]. Particular interest has been devoted to the recently observed decline in BA in tropical regions, mainly in Northern Hemisphere Africa, which has been mostly attributed to the expansion of croplands [82•]. However, other authors have found that cropland expansion in Africa only accounts for 30% of BA reduction, with the rest attributed to increasing net primary productivity [84, 85]. The analysis of agricultural fires is particularly challenging since they tend to be small and low intensity and are therefore difficult to map using standard RS approaches [86]. However, considering these cropland fires are important to better account for atmospheric emissions, particularly in some regions where they have a relevant impact on air pollution [87, 88].

A growing recent trend in RS of fire effects is the use of BA products for parameterization of Dynamic Global Vegetation Models (DGVM). Most DGVM include a fire component, which tries to estimate the impact of fire over vegetation and soils [89]. These fire modules generally use stochastic processes to estimate fire ignition and standard fire propagation models to estimate BA [90•]. Several studies have found a tendency towards underestimation of actual BA by these models [91]. For this reason, recent studies tried to improve them by better understanding the spatial variation of fire characteristics. The most analysed in the last few years are fire size, shape, and orientation [92]. As a first step, those studies require the conversion of BA products to single fire events. Several methods have been proposed with this aim, including flooding algorithms [83] and fire propagation simulations [93]. Other authors have used neighbourhood algorithms to create fire clusters from thermal anomalies [94]. Once fire events have been individualized, several analyses can be conducted, such as fire-size distribution [83, 95], or relations between fire size and fire radiative power [96]. In addition, the use of BA products in DGVM requires a better characterization of product uncertainty, which is a novel field of research that requires further efforts [97].

The relations between fire occurrence and atmospheric emissions have been widely analysed, both using bottom-up approaches, considering BA, biomass loss, and emission factors [98•, 99] and using top-down approaches, based on atmospheric sensors measuring several gases associated with fire emissions, such as CO, CO2, CH4, or NH3 [71]. Regional studies linking fire occurrence and atmospheric emissions have been carried out in several continents: Europe [100], China [101], and Mexico [47].

Analysis of global BA products has also found interesting connections between fire activity and other biophysical variables. For instance, Boreal fire activity has been linked to albedo and snow changes in Western US [102], Greenland [48], and the Arctic [103]. Global impacts of fire on surface temperature vary along the latitudes, with net cooling in the Boreal regions and net warming in the Tropics [104]. The latest studies have also analysed the relations of BA and albedo trends [105] and BA and mass movements [106].

In addition to generating and analysing global BA products, many recent studies continue developing regional or local BA products, generally from medium-resolution sensors. Particular interest has been devoted to areas sensitive to periodic droughts, such as the Amazon basin [107] or the South African region [108]. Proposals of new or adapted BA algorithms have been done, mostly in refining change detection techniques (Brazil [109], Canada [110], and Northwestern USA [111]) and incorporating different machine learning approaches, such as random forest [112], genetic programming [113], support vector machines [114], or neural networks [115]. OBIA analysis has also been widely used for BA classification [114, 116]. Machine learning approaches have been used as well for the selection of input variables for BA discrimination [3]. In spite of the growing interest in these automatic approaches, physical-based BA algorithms are still widely used. The most commonly used is a two-phase approach, which aims first to detect the most clearly burned pixels and then apply spatial analysis to improve the determination of the fire patch [79•, 117, 118].

These regional or local studies have frequently used new sensors, such as Sentinel-2 [75•, 119, 120], AWIFS data on board Indian satellites [121], high-resolution satellites, such as Worldview images [122] or the Chinese HJ satellites [123], and unmanned aerial vehicles [124]. Medium-resolution sensors, such as those on board the Sentinel-2 or Landsat satellites, provide a much more detailed assessment of small fires than standard global BA products. A recent comparison between S-2 and MODIS products over Africa revealed that 80% of total BA in the continent was missed by the MODIS product, mainly due to omissions of fires < 100 ha [75•]. Improvements in computation power may provide in the near future global BA products based on medium-resolution

sensors. A prototype global BA product based on Landsat-8 images has been recently published [125].

The growing availability of radar images as a result of the Sentinel-1 satellites has extended the development of SAR-based BA algorithms [2•, 126, 127]. They have shown particular interest in cloudy areas of the Tropics. Since the physical basis of radar acquisition is quite complex, the development of conceptual models based on physical approaches facilitates the generalization of those models [128]. In addition to C-band algorithms (such as those adapted to Sentinel-1 or ERS data), other authors have worked in other microwave bands, such as the X [129] and L bands [130, 131], which provide complementary information on forest canopy and understory, respectively.

Several authors have noted the relevance of integrating different medium-resolution sensors to improve temporal coverage. Combined use of these medium-resolution sensors improves the detection of low persistence burn signals [132, 133]. Several studies comparing optical and radar BA detection have also been recently published [5, 134].

Both global and regional BA products are useful when they are accurate, both in terms of BA detection and temporal reporting. Validation of global BA products is particularly challenging, as it requires a large effort to provide statistically significant estimations. Following standard validation protocols, the FireCCI project initiated different validation exercises, first using a single year [135, 136] and later using a temporal series [78]. In both cases, samples were derived from stratified random sampling, using as strata global biomes and spatial and seasonal occurrence. Average omission and commission errors of the most accurate global BA products were estimated as 62 and 35%, respectively. Errors were mostly associated with missing small fires. Different studies have compared MODIS and Landsat BA products for specific regions: Brazil [137], China [138], and the USA [139]. They confirmed high omission rates for global products, particularly for fires smaller than 40 ha. In Florida, with 92% of all BA in prescribed burnings, the omissions of BA products were found particularly relevant [140].

The validation of medium-resolution BA products implicates additional challenges, as it requires generating reference datasets from high-resolution images, which are expensive and difficult to access. As an alternative, some of these validation studies were derived from independently interpreted medium-resolution data. For instance, in the USA Conus area, comparison of a Landsat-based BA product with visually controlled Landsat reference sites offered omission and commission errors of 42 and 33% [141]. The same authors developed another validation exercise using high-resolution images (Quickbird, Geoeye), finding omission, and commission errors of 22 and 48% [142]. As it is the case of global BA products, these Landsat-derived BA maps found higher errors for agricultural regions, as tilled areas were sometimes confused with BA pixels. A few intercomparison studies have also been published in the last years, linking spatial and temporal trends of BA products [143]. Regional comparisons have also been developed in Africa [144].

Fire is not a binary process, and therefore, the analysis of fire impacts requires better discrimination of variations of burn severity. RS methods provide a comprehensive view of post-fire variations, but they are not necessarily related to fire impacts on plants and soils. This topic has been extensively covered in the last two decades, particularly after the development of the Monitoring Trends in Burn Severity (MTBS) program in the US (https://www.mtbs.gov/), which provides burn severity information for all fires larger than a certain threshold based on Landsat multitemporal analysis. The basic indices developed for this program have been extended with additional proposals, in different ecosystems: Eastern Siberia [145], California [146, 147], or Western US [148]. Some papers have tried to provide a more ecological sound interpretation of satellite-retrieved burn severity, using a Random Forest model [149•]; others have combined passive optical with lidar data to detect the relevance of post-fire legacies in vegetation height and biomass [150, 151] or in the distribution of snags of different sizes [152]. Fuel consumption has been estimated from active fire and fire radiative power [153] or from vegetation optical depth obtained from microwave data [154]. Even though the use of radiative transfer models for estimating burn severity provided sound results in different ecosystems [155], it has not been greatly covered in the last few years.

Monitoring Post-Fire Recovery

Forest fires are one of the most common disturbance types around the world. For this reason, characterizing fire disturbance and monitoring post-fire regeneration are relevant topics both for ecological and management purposes. Chu et al. [156••] and Bartels et al. [157] provided a review of concepts, methods, and sensors related to this subject.

Post-fire recovery analysis should be connected to a clear comprehension of ecological drivers that influence the recovery processes [158]. In this sense, post-fire regeneration depends on biotic and abiotic factors, but little is still known about how these factors interact in natural recovery processes after fire disturbance. Several studies have used geographical variables (topography, soil characteristics, or climate) as drivers of post-fire vegetation recovery [159–161], while some others have emphasized the relevance of burn severity to characterize regeneration patterns [162–164]. The legacy effects have also been analysed [150, 157], as well as forest composition before the fire [165]. Spatial properties of the landscape, such as nearest distance to unburned area, a proxy

of edge effect, or tree species characteristics have also been identified as key drivers of recovery [166, 167]. The relative importance of these variables and their interaction in the wildfire regeneration process remains still largely unknown.

One recent trend in monitoring fire recovery is based on using long time series of RS data, especially since 2008 when the US Geological Survey (USGS) opened access to the Landsat archive. This fact has accelerated the analysis of historical trends, and it has incremented the numbers of methods and applications to characterize the ecosystem response to forest fires. One of the pioneers of these temporal analyses, Kennedy [158] has spoken about "a new paradigm in remote sensing of landscape change". Following these ideas, a range of algorithms have been developed and applied to Landsat time series (LTS). The most extended are [168] as follows: the Vegetation Change Tracker (VCT), designed to monitor forest disturbance history with LTS, which was used by Zhao et al. [169] to detect wildfire in North America; the Continuous Change Detection and Classification (CCDC), developed by Zhu et al. [170] to identify land cover changes; and the Composite2Change (C2C), a trajectory pixel algorithm, developed by Hermosilla et al. [171] to detect forest disturbance in Canada, by analysing changes in the different disturbances of the country for past 25 years [172•]. However, still the most extended algorithm for time series analysis of Landsat data is the Landsat-based Detection of Trends in Disturbance and Recovery (LandTrendr) [173]· [159, 174]. LandTrendr was specifically designed to be used with Landsat data, but it might be adapted to Sentinel-2 to extend the baseline data. In addition, this algorithm has been recently adapted to Google Earth Engine (GEE), thus facilitating the characterization of large areas over long periods of time [175]. All these algorithms are pixel based, while recently a novel patch-based approach, Vegetation Regeneration and Disturbance Estimates through Time (VeRDET), have been developed to detect periods of vegetation disturbance, stability, and growth from the historical Landsat image records [176].

In terms of input data for running these time change algorithms, the most common have been the spectral vegetation indexes (SVI) such as NDVI (normalized ratio of red and near infrared reflectance), NBR (ratio of near infrared and SWIR reflectance) and its derivatives dNBR, RdNBR, and the components of the Tasselled Cap Transformation [159, 177]. There is not a clear consensus on what indexes are more adequate to analyse vegetation recovery after fire. Morresi et al. [178] recommended using NDVI, which mostly captures chlorophyll concentration and canopy greenness, for tracking early stages of the secondary succession in the Central Appennines (Italy). Storey et al. [179] also used NDVI to estimate forest recovery up to 12 years in chamise chaparral (California), which was related to grassland or shrubland cover during the early recovery process. The NBR, which mainly responds to moisture variations in leaves, has been successfully used to detect and classify disturbance in Canada [172•, 180]. Massetti et al. [181] developed a new index VSPI (Vegetation Structure Perpendicular Index) for vegetation recovery that outperformed the NDVI and NBR. This index is based on the divergence from a linear regression between two SWIR bands, and it has showed a minor inter-annual variability and stronger post-fire monitoring of disturbance over a longer period in Australian eucalypts forest. However, several studies recommend to combine several SVI, applying each one to different stages of the forest recovery process [182–184]. Furthermore, it would be convenient to understand better the advantages and limitations of these indices when interpreting RS data, in the context of post-fire regeneration [174, 182].

Lidar data have also been use to estimate post-fire changes in forest structure. Matasci et al. [185] combined lidar and Landsat data using a nearest neighbour imputation approach with a Random Forest-based distance metric to estimate height, basal area, volume, and biomass changes in the Canadian forest, for the period 1984–2016. These estimations were used to derive annual forest structure dynamics detecting both undisturbed and regenerating stands after disturbances. Radar can also be useful to assess post-fire regeneration since backscattered microwave energy has proven to be sensitive for detecting changes in vegetation structure. Radar sensors have the advantage over lidar of having different satellite systems in place, particularly Sentinel-1, which provides systematic global coverage. However, only a few studies have been conducted with radar data for assessing post-fire forest dynamics. Chen et al. [186] compared different restoration treatments including natural regeneration using ALOS/PALSAR backscattering coefficients and two radar indices with good results. On the other hand, Polychronaki et al. [187•] combined NDVI index and ERS backscatter coefficients to study the effect of forest fires in a Mediterranean area. They found that radar data could provide information related to changes in dense regeneration coniferous forest, whereas the NDVI was sensitive to the understory vegetation recovery.

Conclusions

This review has identified the main research trends of the last few years for using RS methods to retrieve critical fire information. Fuel moisture content, fuel type mapping, detection of active fires, burned area, and vegetation recovery have been the most common variables generated from RS imagery. To meet the user requirements from sensors that have not been specifically designed for fire applications, many studies combine different sensors and systems, from optical-lidar and radar to thermal-optical. Different spatial and temporal scales have also been linked in the last few years, moving towards

a more comprehensive assessment of fire danger and fire effect assessment. In addition, a growing use of RS products by carbon and atmospheric modellers implies a clear interest about complementing models and observations.

Funding Information No funding was received for this particular review, but support research was funded by the European Space Agency's Climate Change Initiative Programme to Dr. Chuvieco.

Compliance with Ethical Standards

Conflict of Interest The authors declare that they have no conflict of interest.

Human and Animal Rights and Informed Consent This article does not contain any studies with human or animal subjects performed by any of the authors.

References

Papers of particular interest, published recently, have been highlighted as:
- • Of importance
- •• Of major importance

1. Chuvieco E. Editor. Earth observation of wildland fires in Mediterranean ecosystems. Berlin Heidelberg: Springer; 2009.
2.• Belenguer-Plomer MA, Tanase MA, Fernandez-Carrillo A, Chuvieco E. Burned area detection and mapping using Sentinel-1 backscatter coefficient and thermal anomalies. RSE. 2019;233:111345. https://doi.org/10.1016/j.rse.2019.111345 **Description of a comprehensive BA algorithm based on radar images.**
3. Ramo R, García M, Rodríguez D, Chuvieco E. A data mining approach for global burned area mapping. Int J Appl Earth Obs Geoinf. 2018;73:39–51. https://doi.org/10.1016/j.jag.2018.05.027.
4. Giglio L, Loboda T, Roy DP, Quayle B, Justice CO. An active-fire based burned area mapping algorithm for the MODIS sensor. RSE. 2009;113(2):408–20.
5. Stroppiana D, Azar R, Calò F, Pepe A, Imperatore P, Boschetti M, et al. Integration of optical and SAR data for burned area mapping in Mediterranean regions. Remote Sens. 2015;7(2):1320–45.
6. Garcia M, Riano D, Chuvieco E, Salas J, Danson FM. Multispectral and LiDAR data fusion for fuel type mapping using Support Vector Machine and decision rules. RSE. 2011;115(6):1369–79. https://doi.org/10.1016/j.rse.2011.01.017.
7. Yebra M, Dennison P, Chuvieco E, Riaño D, Zylstra P, Hunt ER, et al. A global review of remote sensing of live fuel moisture content for fire danger assessment: moving towards operational products. RSE. 2013;136:455–68. https://doi.org/10.1016/j.rse.2013.05.029.
8. Hislop S, Jones S, Soto-Berelov M, Skidmore A, Haywood A, Nguyen TH. A fusion approach to forest disturbance mapping using time series ensemble techniques. RSE. 2019;221:188–97. https://doi.org/10.1016/j.rse.2018.11.025.
9. Luo K, Quan X, He B, Yebra M. Effects of live fuel moisture content on wildfire occurrence in fire-prone regions over Southwest China. Forests. 2019;10(10):887.
10. Nolan RH, Boer MM, Resco de Dios V, Caccamo G, Bradstock RA. Large-scale, dynamic transformations in fuel moisture drive wildfire activity across Southeastern Australia. Geophys Res Lett. 2016;43(9):4229–38.
11. Pimont F, Ruffault J, Martin-StPaul N, Dupuy J-L. A cautionary note regarding the use of cumulative burnt areas for the determination of fire danger index breakpoints. IJWF. 2019;28(3):254–8.
12.• Yebra M, Quan X, Riaño D, Larraondo PR, van Dijk AI, Cary GJ. A fuel moisture content and flammability monitoring methodology for continental Australia based on optical remote sensing. RSE. 2018;212:260–72 **A practical application of a RS product used for fire risk estimation at national level.**
13. Konings AG, Rao K, Steele-Dunne SC. Macro to micro: microwave remote sensing of plant water content for physiology and ecology. New Phytol. 2019;223(3):1166–72. https://doi.org/10.1111/nph.15808.
14. Wang L, Quan X, He B, Yebra M, Xing M, Liu X. Assessment of the dual polarimetric sentinel-1A data for forest fuel moisture content estimation. Remote Sens. 2019;11(13):1568.
15. Jia S, Kim SH, Nghiem SV, Kafatos M. Estimating live fuel moisture using SMAP L-band radiometer soil moisture for Southern California, USA. Remote Sens. 2019;11(13):1575.
16. Ruffault J, Martin-StPaul N, Pimont F, Dupuy J-L. How well do meteorological drought indices predict live fuel moisture content (LFMC)? An assessment for wildfire research and operations in Mediterranean ecosystems. Agric For Meteorol. 2018;262:391–401. https://doi.org/10.1016/j.agrformet.2018.07.031.
17. Jolly WM, Johnson DM. Pyro-ecophysiology: shifting the paradigm of live Wildland fuel research. Fire. 2018;1(1):8.
18. Nolan RH, Hedo J, Arteaga C, Sugai T, Resco de Dios V. Physiological drought responses improve predictions of live fuel moisture dynamics in a Mediterranean forest. Agric For Meteorol. 2018;263:417–27. https://doi.org/10.1016/j.agrformet.2018.09.011.
19. Yebra M, Scortechini G, Badi A, Beget ME, Boer MM, Bradstock R, et al. Globe-LFMC, a global plant water status database for vegetation ecophysiology and wildfire applications. Sci Data. 2019;6(1):155. https://doi.org/10.1038/s41597-019-0164-9.
20. Pyne SJ, Andrews PL, Laven RD. Introduction to wildland fire. 2nd ed. New York: Wiley; 1996.
21. Chuvieco E. Wildland fire danger estimation and mapping. Singapore: The Role of Remote Sensing Data. World Scientific Publishing; 2003.
22. Albini FA. Estimating wildfire behavior and effects. Gen. Tech. Rep. INT-GTR-30. Ogden: U.S. Department of Agriculture, Forest Service, Intermountain Forest and Range Experiment Station. 92 p; 1976.
23. Wotton BM, Alexander ME, Taylor SW. Updates and Revisions to the 1992 Canadian Forest Fire Behavior Prediction System. Ontario. Information Report GLC-X-10, 45p.: Natural Resources Canada, Canadian Forest Service, Great Lakes Forestry Centre, Sault Ste. Marie; 2009.
24. García M, Popescu S, Riaño D, Zhao K, Neuenschwander A, Agca M, et al. Characterization of canopy fuels using ICESat/GLAS data. RSE. 2012;123(6):81–9. https://doi.org/10.1016/j.rse.2012.03.018.
25. Liu L, Lim S, Shen X, Yebra M. A hybrid method for segmenting individual trees from airborne lidar data. Comput Electron Agric. 2019;163:104871.
26. Bright BC, Hudak AT, Meddens AJH, Hawbaker TJ, Briggs JS, Kennedy RE. Prediction of forest canopy and surface fuels from Lidar and satellite time series data in a bark beetle-affected forest. Forests. 2017;8(9):322. https://doi.org/10.3390/f8090322.
27. García M, Saatchi S, Casas A, Koltunov A, Ustin SL, Ramirez C, et al. Extrapolating Forest canopy fuel properties in the California rim fire by combining airborne LiDAR and Landsat OLI data. Remote Sens. 2017;9(4):394.

28. González-Ferreiro E, Arellano-Pérez S, Castedo-Dorado F, Hevia A, Vega JA, Vega-Nieva D, et al. Modelling the vertical distribution of canopy fuel load using national forest inventory and low-density airborne laser scanning data. PLoS One. 2017;12(4): e0176114. https://doi.org/10.1371/journal.pone.0176114.
29. Romero Ramirez FJ, Navarro-Cerrillo RM, Varo-Martínez MÁ, Quero JL, Doerr S, Hernández-Clemente R. Determination of forest fuels characteristics in mortality-affected Pinus forests using integrated hyperspectral and ALS data. Int J Appl Earth Obs Geoinf. 2018;68:157–67. https://doi.org/10.1016/j.jag.2018.01.003.
30. Marselis SM, Yebra M, Jovanovic T, van Dijk AI. Deriving comprehensive forest structure information from mobile laser scanning observations using automated point cloud classification. Environ Model Softw. 2016;82:142–51.
31. Chen Y, Zhu X, Yebra M, Harris S, Tapper N. Development of a predictive model for estimating forest surface fuel load in Australian eucalypt forests with LiDAR data. Environ Model Softw. 2017;97:61–71.
32. Richter K, Stelling N, Maas HG. Correcting attenuation effects caused by interactions in the forest canopy in full-waveform airborne laser scanner data. Int Arch Photogramm Remote Sens Spat Inf Sci. 2014;XL-3:273–80. https://doi.org/10.5194/isprsarchives-XL-3-273-2014.
33. Alonso-Benito A, Arroyo LA, Arbelo M, Hernandez-Leal P. Fusion of WorldView-2 and LiDAR data to map fuel types in the Canary Islands. Remote Sens. 2016;8(8):669. https://doi.org/10.3390/rs8080669.
34. García M, Riaño D, Chuvieco E, Salas J, Danson FM. Multispectral and LiDAR data fusion for fuel type mapping using Support Vector Machine and decision rules. Remote Sens Environ. 2011;115(6):1369–79. https://doi.org/10.1016/j.rse.2011.01.017 **Combined use of Lidar and passive optical sensors for fuel type mapping.**
35. Marino E, Ranz P, Tome JL, Noriega MA, Esteban J, Madrigal J. Generation of high-resolution fuel model maps from discrete airborne laser scanner and Landsat-8 OLI: a low-cost and highly updated methodology for large areas. Remote Sens Environ. 2016;187:267–80. https://doi.org/10.1016/j.rse.2016.10.020.
36. Stavros EN, Coen J, Peterson B, Singh H, Kennedy K, Ramirez C, et al. Use of imaging spectroscopy and LIDAR to characterize fuels for fire behavior prediction. Remote Sens Appl Soc Environ. 2018;11:41–50. https://doi.org/10.1016/j.rsase.2018.04.010.
37. Sanchez YS, Martinez-Grana A, Frances FS, Picado MM. Mapping wildfire ignition probability using Sentinel 2 and LiDAR (Jerte Valley, Caceres, Spain). Sensors. 2018;18(3):826. https://doi.org/10.3390/s18030826.
38. García M, Saatchi S, Ustin S, Balzter H. Modelling forest canopy height by integrating airborne LiDAR samples with satellite radar and multispectral imagery. Int J Appl Earth Obs Geoinf. 2018;66: 159–73.
39. Stefanidou A, Dragozi E, Stavrakoudis D, Gitas IZ. Fuel type mapping using object-based image analysis of DMC and Landsat-8 OLI imagery. Geocarto Int. 2018;33(10):1064–83. https://doi.org/10.1080/10106049.2017.1333532.
40. Bajocco S, Dragoz E, Gitas I, Smiraglia D, Salvati L, Ricotta C. Mapping forest fuels through vegetation phenology: the role of coarse-resolution satellite time-series. PLoS One. 2015;10(3): e0119811. https://doi.org/10.1371/journal.pone.0119811.
41. Flannigan MD, Vonder Haar TH. Forest fire monitoring using NOAA satellite AVHRR. Can J For Res. 1986;16:975–82.
42. Dwyer E, Pereira JMC, Grégorie J-M, DaCamara CC. Characterization of the spatio-temporal patterns of global fire activity using satellite imagery for the period April 1992 to March 1993. J Biogeogr. 2000;27(1):57–69. https://doi.org/10.1046/j.1365-2699.2000.00339.x.
43. Lizundia-Loiola J, Pettinari ML, Chuvieco E. Temporal anomalies in burned area trends: satellite estimations of the Amazonian 2019 Fire Crisis. Remote Sens. 2020;12(1):151. https://doi.org/10.3390/rs12010151.
44. Baker KR, Woody MC, Valin L, Szykman J, Yates EL, Iraci LT, et al. Photochemical model evaluation of 2013 California wild fire air quality impacts using surface, aircraft, and satellite data. Sci Total Environ. 2018;637:1137–49. https://doi.org/10.1016/j.scitotenv.2018.05.048.
45. Duc HN, Chang LTC, Azzi M, Jiang NB. Smoke aerosols dispersion and transport from the 2013 New South Wales (Australia) bushfires. Environ Monit Assess. 2018;190(7):428. https://doi.org/10.1007/s10661-018-6810-4.
46. Adams C, McLinden CA, Shephard MW, Dickson N, Dammers E, Chen J, et al. Satellite-derived emissions of carbon monoxide, ammonia, and nitrogen dioxide from the 2016 Horse River wildfire in the Fort McMurray area. Atmos Chem Phys. 2019;19(4): 2577–99. https://doi.org/10.5194/acp-19-2577-2019.
47. Cruz-López MI, Manzo-Delgado LDL, Aguirre-Gómez R, Chuvieco E, Equihua-Benítez JA. Spatial distribution of forest fire emissions: a case study in three Mexican ecoregions. Remote Sens. 2019;11(10):1185.
48. Evangeliou N, Kylling A, Eckhardt S, Myroniuk V, Stebel K, Paugam R, et al. Open fires in Greenland in summer 2017: transport, deposition and radiative effects of BC, OC and BrC emissions. Atmos Chem Phys. 2019;19(2):1393–411. https://doi.org/10.5194/acp-19-1393-2019.
49. Coen JL, Stavros EN, Fites-Kaufman JA. Deconstructing the King megafire. Ecol Appl. 2018;28(6):1565–80. https://doi.org/10.1002/eap.1752.
50. Pinto RMS, Benali A, Sa ACL, Fernandes PM, Soares PMM, Cardoso RM, et al. Probabilistic fire spread forecast as a management tool in an operational setting. Springerplus. 2016;5:Unsp 1205. https://doi.org/10.1186/s40064-016-2842-9.
51. Anejionu OCD, Blackburn GA, Whyatt JD. Detecting gas flares and estimating flaring volumes at individual flow stations using MODIS data. RSE. 2015;158:81–94. https://doi.org/10.1016/j.rse.2014.11.018.
52. Marchese F, Neri M, Falconieri A, Lacava T, Mazzeo G, Pergola N, et al. The contribution of multi-sensor infrared satellite observations to monitor Mt. Etna (Italy) activity during May to August 2016. Remote Sens. 2018;10(12):1948. https://doi.org/10.3390/rs10121948.
53. Wooster MJ, Roberts G, Freeborn PH, Xu W, Govaerts Y, Beeby R, et al. LSA SAF Meteosat FRP products - part 1: algorithms, product contents, and analysis. Atmos Chem Phys. 2015;15(22): 13217–39. https://doi.org/10.5194/acp-15-13217-2015.
54. Hally B, Wallace L, Reinke K, Jones S, Skidmore A. Advances in active fire detection using a multi-temporal method for next-generation geostationary satellite data. Int J Digit Earth. 2019;12(9):1030–45. https://doi.org/10.1080/17538947.2018.1497099.
55. Wickramasinghe C, Wallace L, Reinke K, Jones S. Implementation of a new algorithm resulting in improvements in accuracy and resolution of SEVIRI hotspot products. Remote Sens Lett. 2018;9(9):877–85.
56. Wickramasinghe C, Jones S, Reinke K, Wallace L. Development of a multi-spatial resolution approach to the surveillance of active fire lines using Himawari-8. Remote Sens. 2016;8(11):932.
57.• Giglio L, Schroeder W, Justice CO. The collection 6 MODIS active fire detection algorithm and fire products. RSE. 2016;178: 31–41 **Description of the most widely used fire detection algorithm.**

58. Oliva P, Schroeder W. Assessment of VIIRS 375 m active fire detection product for direct burned area mapping. RSE. 2015;160:144–55.
59. Csiszar I, Schroeder W, Giglio L, Ellicott E, Vadrevu KP, Justice CO, et al. Active fires from the Suomi NPP visible infrared imaging radiometer suite: product status and first evaluation results. J Geophys Res-Atmos. 2014;119(2):803–16. https://doi.org/10.1002/2013jd020453.
60. Lin ZY, Chen F, Niu Z, Li B, Yu B, Jia HC, et al. An active fire detection algorithm based on multi-temporal FengYun-3C VIRR data. RSE. 2018;211:376–87. https://doi.org/10.1016/j.rse.2018.04.027.
61. Schroeder W, Oliva P, Giglio L, Quayle B, Lorenz E, Morelli F. Active fire detection using Landsat-8/OLI data. RSE. 2016;185:210–20.
62. Mitchell S, Jones S, Reinke K, Lorenz E, Reulke R. Assessing the utility of the TET-1 hotspot detection and characterization algorithm for determining wildfire size and temperature. IJRS. 2016;37(20):4731–47. https://doi.org/10.1080/01431161.2016.1204026.
63. Atwood EC, Englhart S, Lorenz E, Halle W, Wiedemann W, Siegert F. Detection and characterization of low temperature peat fires during the 2015 fire catastrophe in Indonesia using a new high-sensitivity fire monitoring satellite sensor (FireBird). PLoS One. 2016;11(8):e0159410. https://doi.org/10.1371/journal.pone.0159410.
64. Schroeder W, Oliva P, Giglio L, Csiszar IA. The new VIIRS 375 m active fire detection data product: algorithm description and initial assessment. RSE. 2014;143:85–96. https://doi.org/10.1016/j.rse.2013.12.008.
65. Noojipady P, Morton DC, Macedo MN, Victoria DC, Huang CQ, Gibbs HK, et al. Forest carbon emissions from cropland expansion in the Brazilian Cerrado biome. Environ Res Lett. 2017;12(2):025004. https://doi.org/10.1088/1748-9326/aa5986.
66. Polivka TN, Wang J, Ellison LT, Hyer EJ, Ichoku CM. Improving nocturnal fire detection with the VIIRS day-night band. IEEE Trans Geosci Remote. 2016;54(9):5503–19. https://doi.org/10.1109/tgrs.2016.2566665.
67. Waigl CF, Prakash A, Stuefer M, Verbyla D, Dennison P. Fire detection and temperature retrieval using EO-1 Hyperion data over selected Alaskan boreal forest fires. Int J Appl Earth Obs Geoinf. 2019;81:72–84. https://doi.org/10.1016/j.jag.2019.03.004.
68. Xia HP, Chen YH, Quan JL. A simple method based on the thermal anomaly index to detect industrial heat sources. Int J Appl Earth Obs Geoinf. 2018;73:627–37. https://doi.org/10.1016/j.jag.2018.08.003.
69. Kato S, Kouyama T, Nakamura R, Matsunaga T, Fukuhara T. Simultaneous retrieval of temperature and area according to subpixel hotspots from nighttime Landsat 8 OLI data. RSE. 2018;204:276–86. https://doi.org/10.1016/j.rse.2017.10.025.
70.• Parker RJ, Boesch H, Wooster MJ, Moore DP, Webb AJ, Gaveau D, et al. Atmospheric CH4 and CO2 enhancements and biomass burning emission ratios derived from satellite observations of the 2015 Indonesian fire plumes. Atmos Chem Phys. 2016;16(15):10111–31. https://doi.org/10.5194/acp-16-10111-2016 **Atmospheric emission estimations from top-down satellite products.**
71. Whitburn S, Van Damme M, Clarisse L, Hurtmans D, Clerbaux C, Coheur PF. IASI-derived NH3 enhancement ratios relative to CO for the tropical biomass burning regions. Atmos Chem Phys. 2017;17(19):12239–52. https://doi.org/10.5194/acp-17-12239-2017.
72. Elvidge CD, Zhizhin M, Hsu FC, Baugh K, Khomarudin MR, Vetrita Y, et al. Long-wave infrared identification of smoldering peat fires in Indonesia with nighttime Landsat data. Environ Res Lett. 2015;10(6):065002. https://doi.org/10.1088/1748-9326/10/6/065002.
73. Sofan P, Bruce D, Jones E, Marsden J. Detection and validation of tropical peatland flaming and smouldering using Landsat-8 SWIR and TIRS Bands. Remote Sens. 2019;11(4):465. https://doi.org/10.3390/rs11040465.
74.•• Chuvieco E, Mouillot F, van der Werf GR, San Miguel J, Tanasse M, Koutsias N, et al. Historical background and current developments for mapping burned area from satellite Earth observation. RSE. 2019;225:45–64. https://doi.org/10.1016/j.rse.2019.02.013 **Recent review paper on burned area methods and products from RS data.**
75.• Roteta E, Bastarrika A, Storm T, Chuvieco E. Development of a Sentinel-2 burned area algorithm: generation of a small fire database for northern hemisphere tropical Africa. RSE. 2019;222(1):1–17. https://doi.org/10.1016/j.rse.2018.12.011 **First continental-scale BA product derived from Sentinel-2 imagery.**
76. Hawbaker TJ, Vanderhoof MK, Beal Y-J, Takacs JD, Schmidt GL, Falgout JT, et al. Mapping burned areas using dense time-series of Landsat data. RSE. 2017;198:504–22.
77.• Giglio L, Boschetti L, Roy DP, Humber ML, Justice CO. The Collection 6 MODIS Burned Area Mapping Algorithm and Product. RSE. 2018;217:72–85 **Description of the BA algorithm used for NASA products.**
78. Chuvieco E, Lizundia-Loiola J, Pettinari ML, Ramo R, Padilla M, Tansey K, et al. Generation and analysis of a new global burned area product based on MODIS 250 m reflectance bands and thermal anomalies. Earth Syst Sci Data. 2018;10:2015–31. https://doi.org/10.5194/essd-10-2015-2018.
79.• Lizundia-Loiola J, Otón G, Ramo R, Chuvieco E. A spatio-temporal active-fire clustering approach for global burned area mapping at 250 m from MODIS data. RSE. 2020;236:111493. https://doi.org/10.1016/j.rse.2019.111493 **Descripcion of the BA algorithm used for FireCCI ESA products.**
80. Otón G, Ramo R, Lizundia-Loiola J, Chuvieco E. Global detection of Long-term (1982–2017) burned area with AVHRR-LTDR data. Remote Sens. 2019;11(18):2079. https://doi.org/10.3390/rs11182079.
81. Abatzoglou JT, Williams AP, Boschetti L, Zubkova M, Kolden CA. Global patterns of interannual climate-fire relationships. Glob Chang Biol. 2018;24(11):5164–75. https://doi.org/10.1111/gcb.14405.
82.• Andela N, Morton DC, Giglio L, Chen Y, van der Werf GR, Kasibhatla PS, et al. A human-driven decline in global burned area. Science. 2017;356(6345):1356–62. https://doi.org/10.1126/science.aal4108 **Global trends in fire occurrence based on NASA BA products.**
83. Hantson S, Lasslop G, Kloster S, Chuvieco E. Anthropogenic effects on global mean fire size. IJWF. 2015;24(5):589–96. https://doi.org/10.1071/WF14208.
84. Earl N, Simmonds I. Spatial and temporal variability and trends in 2001-2016 global fire activity. J Geophys Res-Atmos. 2018;123(5):2524–36. https://doi.org/10.1002/2017jd027749.
85. Zubkova M, Boschetti L, Abatzoglou JT, Giglio L. Changes in fire activity in Africa from 2002 to 2016 and their potential drivers. Geophys Res Lett. 2019;46(13):7643–53. https://doi.org/10.1029/2019gl083469.
86. Hall JV, Loboda TV, Giglio L, McCarty GW. A MODIS-based burned area assessment for Russian croplands: mapping requirements and challenges. RSE. 2016;184:506–21.
87. Vadrevu K, Lasko K. Fire regimes and potential bioenergy loss from agricultural lands in the Indo-Gangetic Plains. J Environ Manag. 2015;148:10–20. https://doi.org/10.1016/j.jenvman.2013.12.026.

88. Wu J, Kong SF, Wu FQ, Cheng Y, Zheng SR, Yan Q, et al. Estimating the open biomass burning emissions in central and eastern China from 2003 to 2015 based on satellite observation. Atmos Chem Phys. 2018;18(16):11623–46. https://doi.org/10.5194/acp-18-11623-2018.
89. Lasslop G, Coppola AI, Voulgarakis A, Yue C, Veraverbeke S. Influence of fire on the carbon cycle and climate. Curr Clim Chang Rep. 2019;5(2):112–23. https://doi.org/10.1007/s40641-019-00128-9.
90.• Hantson S, Arneth A, Harrison SP, Kelley DI, Prentice IC, Rabin SS, et al. The status and challenge of global fire modelling. Biogeosciences. 2016;13(11):3359–75 **Review of fire models included in global vegetation models.**
91. Kloster S, Lasslop G. Historical and future fire occurrence (1850 to 2100) simulated in CMIP5 earth system models. Glob Planet Chang. 2017;150:58–69.
92. Laurent P, Mouillot F, Yue C, Ciais P, Moreno MV, Nogueira JMP. FRY, a global database of fire patch functional traits derived from space-borne burned area products. Sci Data. 2018;5:180132. https://doi.org/10.1038/sdata.2018.132.
93. Andela N, Morton DC, Giglio L, Paugam R, Chen Y, Hantson S, et al. The global fire atlas of individual fire size, duration, speed, and direction. Earth Syst Sci Data. 2019;11:529–52. https://doi.org/10.5194/essd-11-529-2019.
94. Oom D, Silva PC, Bistinas I, Pereira JMC. Highlighting biome-specific sensitivity of fire size distributions to time-gap parameter using a new algorithm for fire event individuation. Remote Sens. 2016;8(8):663. https://doi.org/10.3390/rs8080663.
95. Kantzas EP, Quegan S, Lomas M. Improving the representation of fire disturbance in dynamic vegetation models by assimilating satellite data: a case study over the Arctic. Geosci Model Dev. 2015;8(8):2597–609. https://doi.org/10.5194/gmd-8-2597-2015.
96. Laurent P, Mouillot F, Moreno MV, Yue C, Ciais P. Varying relationships between fire radiative power and fire size at a global scale. Biogeosciences. 2019;16(2):275–88. https://doi.org/10.5194/bg-16-275-2019.
97. Brennan J, Gomez-Dans JL, Disney M, Lewis P. Theoretical uncertainties for global satellite-derived burned area estimates. Biogeosciences. 2019;16(16):3147–64. https://doi.org/10.5194/bg-16-3147-2019.
98.• van der Werf GR, Randerson JT, Giglio L, van Leeuwen TT, Chen Y, Rogers BM, et al. Global fire emissions estimates during 1997–2016. Earth Syst Sci Data. 2017;9:697–720. https://doi.org/10.5194/essd-9-697-2017 **Estimations of fire emissions derived from satellite BA products**.
99. Poulter B, Cadule P, Cheiney A, Ciais P, Hodson E, Peylin P, et al. Sensitivity of global terrestrial carbon cycle dynamics to variability in satellite-observed burned area. Glob Biogeochem Cycles. 2015;29(2):207–22. https://doi.org/10.1002/2013gb004655.
100. Majdi M, Turquety S, Sartelet K, Legorgeu C, Menut L, Kim Y. Impact of wildfires on particulate matter in the Euro-Mediterranean in 2007: sensitivity to some parameterizations of emissions in air quality models. Atmos Chem Phys. 2019;19(2):785–812. https://doi.org/10.5194/acp-19-785-2019.
101. Qiu XH, Duan L, Chai FH, Wang SX, Yu Q, Wang SL. Deriving high-resolution emission inventory of open biomass burning in China based on satellite observations. Environ Sci Technol. 2016;50(21):11779–86. https://doi.org/10.1021/acs.est.6b02705.
102. Gleason KE, McConnell JR, Arienzo MM, Chellman N, Calvin WM. Four-fold increase in solar forcing on snow in western US burned forests since 1999. Nat Commun. 2019;10:2026. https://doi.org/10.1038/s41467-019-09935-y.
103. Monks SA, Arnold SR, Emmons LK, Law KS, Turquety S, Duncan BN, et al. Multi-model study of chemical and physical controls on transport of anthropogenic and biomass burning pollution to the Arctic. Atmos Chem Phys. 2015;15(6):3575–603. https://doi.org/10.5194/acp-15-3575-2015.
104. Liu ZH, Ballantyne AP, Cooper LA. Biophysical feedback of global forest fires on surface temperature. Nat Commun. 2019;10(1):214. https://doi.org/10.1038/s41467-018-08237-z.
105. Mota B, Gobron N, Cappucci F, Morgan O. Burned area and surface albedo products: assessment of change consistency at global scale. RSE. 2019;225:249–66. https://doi.org/10.1016/j.rse.2019.03.001.
106. Ziade R, Abdallah C, Baghdadi N. The effect of forest fire on mass movement in Lebanese mountainous areas. IJWF. 2014;23(6):845–59. https://doi.org/10.1071/wf13077.
107. Gutierrez-Velez VH, Uriarte M, DeFries R, Pinedo-Vasquez M, Fernandes K, Ceccato P, et al. Land cover change interacts with drought severity to change fire regimes in Western Amazonia. Ecol Appl. 2014;24(6):1323–40. https://doi.org/10.1890/13-2101.1.
108. Mayr MJ, Vanselow KA, Samimi C. Fire regimes at the arid fringe: a 16-year remote sensing perspective (2000-2016) on the controls of fire activity in Namibia from spatial predictive models. Ecol Indic. 2018;91:324–37. https://doi.org/10.1016/j.ecolind.2018.04.022.
109. Libonati R, DaCamara CC, Setzer AW, Morelli F, Melchiori AE. An algorithm for burned area detection in the Brazilian Cerrado using 4 gm MODIS imagery. Remote Sens. 2015;7(11):15782–803. https://doi.org/10.3390/rs71115782.
110. Guindon L, Bernier PY, Beaudoin A, Pouliot D, Villemaire P, Hall RJ, et al. Annual mapping of large forest disturbances across Canada's forests using 250 m MODIS imagery from 2000 to 2011. Can J For Res. 2014;44(12):1545–54. https://doi.org/10.1139/cjfr-2014-0229.
111. Sulla-Menashe D, Kennedy RE, Yang ZQ, Braaten J, Krankina ON, Friedl MA. Detecting forest disturbance in the Pacific northwest from MODIS time series using temporal segmentation. RSE. 2014;151:114–23. https://doi.org/10.1016/j.rse.2013.07.042.
112. Ramo R, Chuvieco E. Developing a random Forest algorithm for MODIS global burned area classification. Remote Sens. 2017;9(11):1193.
113. Cabral AIR, Silva S, Silva PC, Vanneschi L, Vasconcelos MJ. Burned area estimations derived from Landsat ETM plus and OLI data: comparing genetic programming with maximum likelihood and classification and regression trees. ISPRS J Photogramm. 2018;142:94–105. https://doi.org/10.1016/j.isprsjprs.2018.05.007.
114. Dragozi E, Gitas IZ, Stavrakoudis DG, Theocharis JB. Burned area mapping using support vector machines and the FuzCoC feature selection method on VHR IKONOS imagery. Remote Sens. 2014;6(12):12005–36. https://doi.org/10.3390/rs61212005.
115. Ba R, Song WG, Li XL, Xie ZX, Lo SM. Integration of multiple spectral indices and a neural network for burned area mapping based on MODIS Data. Remote Sens. 2019;11(3):326. https://doi.org/10.3390/rs11030326.
116. Shimabukuro YE, Miettinen J, Beuchle R, Grecchi RC, Simonetti D, Achard F. Estimating burned area in Mato Grosso, Brazil, using an object-based classification method on a systematic sample of medium resolution satellite images. IEEE J Sel Topics Appl Earth Obs Remote Sens. 2015;8(9):4502–8. https://doi.org/10.1109/jstars.2015.2464097.
117. Alonso-Canas I, Chuvieco E. Global burned area mapping from ENVISAT-MERIS data. RSE. 2015;163:140–52. https://doi.org/10.1016/j.rse.2015.03.011.
118. Hardtke LA, Blanco PD, del Valle HF, Metternicht GI, Sione WF. Semi-automated mapping of burned areas in semi-arid ecosystems using MODIS time-series imagery. Int J Appl Earth Obs Geoinf. 2015;38:25–35. https://doi.org/10.1016/j.jag.2014.11.011.

119. Filipponi F. Exploitation of Sentinel-2 time series to map burned areas at the national level: a case study on the 2017 Italy wildfires. Remote Sens. 2019;11(6):622. https://doi.org/10.3390/rs11060622.
120. Huang HY, Roy DP, Boschetti L, Zhang HKK, Yan L, Kumar SS, et al. Separability analysis of Sentinel-2A Multi-Spectral Instrument (MSI) data for burned area discrimination. Remote Sens. 2016;8(10):873. https://doi.org/10.3390/rs8100873.
121. Reddy CS, Jha CS, Manaswini G, Alekhya V, Pasha SV, Satish KV, et al. Nationwide assessment of forest burnt area in India using Resourcesat-2 AWiFS data. Curr Sci. 2017;112(7):1521–32. https://doi.org/10.18520/cs/v112/i07/1521-1532.
122. Meng R, Wu J, Schwager KL, Zhao F, Dennison PE, Cook BD, et al. Using high spatial resolution satellite imagery to map forest burn severity across spatial scales in a pine barrens ecosystem. RSE. 2017;191:95–109. https://doi.org/10.1016/j.rse.2017.01.016.
123. Liu WL, Wang LT, Zhou Y, Wang SX, Zhu JF, Wang FT. A comparison of forest fire burned area indices based on HJ satellite data. Nat Hazards. 2016;81(2):971–80. https://doi.org/10.1007/s11069-015-2115-x.
124. Fraser RH, van der Sluijs J, Hall RJ. Calibrating satellite-based indices of burn severity from UAV-derived metrics of a burned boreal forest in NWT, Canada. Remote Sens. 2017;9(3):279. https://doi.org/10.3390/rs9030279.
125. Long T, Zhang Z, He G, Jiao W, Tang C, Wu B, et al. 30 m resolution global annual burned area mapping based on Landsat images and Google Earth Engine. Remote Sens. 2019;11(5):489.
126. Lohberger S, Stängel M, Atwood EC, Siegert F. Spatial evaluation of Indonesia's 2015 fire-affected area and estimated carbon emissions using Sentinel-1. Glob Chang Biol. 2018;24:644–54. https://doi.org/10.1111/gcb.13841.
127. Lasaponara R, Tucci B. Identification of burned areas and severity using SAR Sentinel-1. IEEE Geosci Remote Sens Lett. 2019;16(6):917–21. https://doi.org/10.1109/lgrs.2018.2888641.
128. Kalogirou V, Ferrazzoli P, Della Vecchia A, Foumelis M. On the SAR backscatter of burned forests: a model-based study in C-band, Over Burned Pine Canopies. IEEE TransGeosRS. 2014;52(10):6205–15. https://doi.org/10.1109/tgrs.2013.2295594.
129. Bernhard EM, Twele A, Martinis S. The effect of vegetation type and density on X-band SAR backscatter after forest fires. Photogramm Fernerkundung Geoinf. 2014;4:275–85. https://doi.org/10.1127/1432-8364/2014/0222.
130. Fernandez-Carrillo A, McCaw L, Tanase MA. Estimating prescribed fire impacts and post-fire tree survival in eucalyptus forests of Western Australia with L-band SAR data. RSE. 2019;224:133–44. https://doi.org/10.1016/j.rse.2019.02.005.
131. Plank S, Karg S, Martinis S. Full-polarimetric burn scar mapping - the differences of active fire and post-fire situations. IJRS. 2019;40(1):253–68. https://doi.org/10.1080/01431161.2018.1512768.
132. Quintano C, Fernandez-Manso A, Fernandez-Manso O. Combination of Landsat and Sentinel-2 MSI data for initial assessing of burn severity. Int J Appl Earth Obs Geoinf. 2018;64:221–5. https://doi.org/10.1016/j.jag.2017.09.014.
133. Mallinis G, Mitsopoulos I, Chrysafi I. Evaluating and comparing Sentinel 2A and Landsat-8 operational land imager (OLI) spectral indices for estimating fire severity in a Mediterranean pine ecosystem of Greece. GISci Remote Sens. 2018;55(1):1–18.
134. Verhegghen A, Eva H, Ceccherini G, Achard F, Gond V, Gourlet-Fleury S, et al. The potential of Sentinel satellites for burnt area mapping and monitoring in the Congo Basin forests. Remote Sens. 2016;8(12):986.
135. Padilla M, Stehman SV, Hantson S, Oliva P, Alonso-Canas I, Bradley A, et al. Comparing the accuracies of remote sensing global burned area products using stratified random sampling and estimation. RSE. 2015;160:114–21. https://doi.org/10.1016/j.rse.2014.01.008.
136. Padilla M, Stehman SV, Chuvieco E. Validation of the 2008 MODIS-MCD45 global burned area product using stratified random sampling. RSE. 2014;144:187–96. https://doi.org/10.1016/j.rse.2014.01.008.
137. Alves DB, Perez-Cabello F, Mimbrero MR, Febrer-Martinez M. Accuracy assessment of the latest generations of MODIS burned area products for mapping fire scars on a regional scale over Campos Amazonicos Savanna Enclave (Brazilian Amazon). J Appl Remote Sens. 2018;12(2):026026. https://doi.org/10.1117/1.jrs.12.026026.
138. Fornacca D, Ren GP, Xiao W. Performance of Three MODIS Fire Products (MCD45A1, MCD64A1, MCD14ML), and ESA Fire_CCI in a Mountainous Area of Northwest Yunnan, China, Characterized by Frequent Small Fires. Remote Sens. 2017;9(11):1131. https://doi.org/10.3390/rs9111131.
139. Mangeon S, Field R, Fromm M, McHugh C, Voulgarakis A. Satellite versus ground-based estimates of burned area: a comparison between MODIS based burned area and fire agency reports over North America in 2007. Anthropocene Rev. 2016;3(2):76–92.
140. Nowell HK, Holmes CD, Robertson K, Teske C, Hiers JK. A new picture of fire extent, variability, and drought interaction in prescribed fire landscapes: insights from Florida government records. Geophys Res Lett. 2018;45(15):7874–84. https://doi.org/10.1029/2018gl078679.
141. Vanderhoof MK, Fairaux N, Beal Y-JG, Hawbaker TJ. Validation of the USGS Landsat burned area essential climate variable (BAECV) across the conterminous United States. RSE. 2017;198:393–406.
142. Vanderhoof MK, Brunner N, Beal Y-JG, Hawbaker TJ. Evaluation of the US geological survey Landsat burned area essential climate variable across the conterminous US using commercial high-resolution imagery. Remote Sens. 2017;9(7):743.
143. Humber ML, Boschetti L, Giglio L, Justice CO. Spatial and temporal intercomparison of four global burned area products. Int J Digit Earth. 2019;12(4):460–84.
144. Freeborn PH, Cochrane MA, Wooster MJ. A decade Long, multi-scale map comparison of fire regime parameters derived from three publically available satellite-based fire products: a case study in the Central African Republic. Remote Sens. 2014;6(5):4061–89. https://doi.org/10.3390/rs6054061.
145. Kurbanov E, Vorobyev O, Leznin S, Polevshikova Y, Demisheva E. Assessment of burn severity in middle Povozhje with Landsat multitemporal data. IJWF. 2017;26(9):772–82. https://doi.org/10.1071/wf16141.
146. Miller JD, Safford HD, Welch KR. Using one year post-fire fire severity assessments to estimate longer term effects of fire in conifer forests of northern and eastern California, USA. For Ecol Manag. 2016;382:168–83. https://doi.org/10.1016/j.foreco.2016.10.017.
147. Meddens AJH, Kolden CA, Lutz JA. Detecting unburned areas within wildfire perimeters using Landsat and ancillary data across the northwestern United States. RSE. 2016;186:275–85. https://doi.org/10.1016/j.rse.2016.08.023.
148. Zheng Z, Zeng YN, Li SN, Huang W. A new burn severity index based on land surface temperature and enhanced vegetation index. Int J Appl Earth Obs Geoinf. 2016;45:84–94. https://doi.org/10.1016/j.jag.2015.11.002.
149.• Parks SA, Holsinger LM, Koontz MJ, Collins L, Whitman E, Parisien MA, et al. Giving ecological meaning to satellite-derived fire severity metrics across North American Forests. Remote Sens. 2019;11(14):1735. https://doi.org/10.3390/

rs11141735 **Ecological interpretation of fire severity products based on RS data analysis.**

150. Hoffman KM, Trant AJ, Nijland W, Starzomski BM. Ecological legacies of fire detected using plot-level measurements and LiDAR in an old growth coastal temperate rainforest. For Ecol Manag. 2018;424:11–20. https://doi.org/10.1016/j.foreco.2018.04.020.
151. Sato LY, Gomes VCF, Shimabukuro YE, Keller M, Arai E, Nara dos Santos M, et al. Post-fire changes in forest biomass retrieved by airborne LiDAR in Amazonia. Remote Sens. 2016;8(10):839. https://doi.org/10.3390/rs8100839.
152. Vogeler JC, Yang ZQ, Cohen WB. Mapping post-fire habitat characteristics through the fusion of remote sensing tools. RSE. 2016;173:294–303. https://doi.org/10.1016/j.rse.2015.08.011.
153. Andela N, van der Werf GR, Kaiser JW, van Leeuwen TT, Wooster MJ, Lehmann CER. Biomass burning fuel consumption dynamics in the tropics and subtropics assessed from satellite. Biogeosciences. 2016;13(12):3717–34. https://doi.org/10.5194/bg-13-3717-2016.
154. Chen X, Liu YY, Evans JP, Parinussa RM, van Dijk A, Yebra M. Estimating fire severity and carbon emissions over Australian tropical savannahs based on passive microwave satellite observations. IJRS. 2018;39(20):6479–98. https://doi.org/10.1080/01431161.2018.1460507.
155. De Santis A, Chuvieco E, Vaughan P. Short-term assessment of burn severity using the inversion of PROSPECT and GeoSail models. RSE. 2009;113:126–36.
156.•• Chu T, Guo X. Remote sensing techniques in monitoring post-fire effects and patterns of forest recovery in Boreal forest regions: a review. Remote Sens. 2014;6(1):470 **Review of papers on vegetation recovery after fire**.
157. Bartels SF, Chen HYH, Wulder MA, White JC. Trends in post-disturbance recovery rates of Canada's forests following wildfire and harvest. For Ecol Manag. 2016;361:194–207. https://doi.org/10.1016/j.foreco.2015.11.015.
158. Kennedy RE, Andrefouet S, Cohen WB, Gomez C, Griffiths P, Hais M, et al. Bringing an ecological view of change to Landsat-based remote sensing. Front Ecol Environ. 2014;12(6):339–46. https://doi.org/10.1890/130066.
159. Bright BC, Hudak AT, Kennedy RE, Braaten JD, Khalyani AH. Examining post-fire vegetation recovery with Landsat time series analysis in three western North American forest types. Fire Ecol. 2019;15:Unsp 8. https://doi.org/10.1186/s42408-018-0021-9.
160. Ireland G, Petropoulos GP. Exploring the relationships between post-fire vegetation regeneration dynamics, topography and burn severity: a case study from the montane cordillera Ecozones of Western Canada. Appl Geogr. 2015;56:232–48. https://doi.org/10.1016/j.apgeog.2014.11.016.
161. Meng R, Dennison PE, D'Antonio CM, Moritz MA. Remote sensing analysis of vegetation recovery following short-interval fires in Southern California shrublands. PLoS One. 2014;9(10):e110637. https://doi.org/10.1371/journal.pone.0110637.
162. Gordon CE, Price OF, Tasker EM. Mapping and exploring variation in post-fire vegetation recovery following mixed severity wildfire using airborne LiDAR. Ecol Appl. 2017;27(5):1618–32. https://doi.org/10.1002/eap.1555/full.
163. Li XD, Zhang HY, Yang GB, Ding YL, Zhao JJ. Post-fire vegetation succession and surface energy fluxes derived from remote sensing. Remote Sens. 2018;10(7):1000. https://doi.org/10.3390/rs10071000.
164. Shvetsov EG, Kukavskaya EA, Buryak LV, Barrett K. Assessment of post-fire vegetation recovery in Southern Siberia using remote sensing observations. Environ Res Lett. 2019;14(5):055001. https://doi.org/10.1088/1748-9326/ab083d.
165. Lydersen JM, North MP, Collins BM. Severity of an uncharacteristically large wildfire, the rim fire, in forests with relatively restored frequent fire regimes. For Ecol Manag. 2014;328:326–34. https://doi.org/10.1016/j.foreco.2014.06.005.
166. Fang L, Crocker EV, Yang J, Yan Y, Yang YZ, Liu ZH. Competition and burn severity determine post-fire sapling recovery in a nationally protected Boreal forest of China: an analysis from very high-resolution satellite imagery. Remote Sens. 2019;11(6):603. https://doi.org/10.3390/rs11060603.
167. Christopoulou A, Mallinis G, Vassilakis E, Farangitakis GP, Fyllas NM, Kokkoris GD, et al. Assessing the impact of different landscape features on post-fire forest recovery with multitemporal remote sensing data: the case of Mount Taygetos (southern Greece). Int J Wildland Fire. 2019;28(7):521–32. https://doi.org/10.1071/wf18153.
168. Hirschmugl M, Gallaun H, Dees M, Datta P, Deutscher J, Koutsias N, et al. Methods for mapping forest disturbance and degradation from optical earth observation data: a review. Curr For Rep. 2017;3(1):32–45. https://doi.org/10.1007/s40725-017-0047-2.
169. Zhao FR, Meng R, Huang CQ, Zhao MS, Zhao FA, Gong P, et al. Long-term post-disturbance forest recovery in the greater yellowstone ecosystem analyzed using Landsat time series stack. Remote Sens. 2016;8(11):Unsp 898. https://doi.org/10.3390/rs8110898.
170. Zhu Z, Woodcock CE. Continuous change detection and classification of land cover using all available Landsat data. Remote Sens Environ. 2014;144:152–71. https://doi.org/10.1016/j.rse.2014.01.011.
171. Hermosilla T, Wulder MA, White JC, Coops NC, Hobart GW. Regional detection, characterization, and attribution of annual forest change from 1984 to 2012 using Landsat-derived time-series metrics. Remote Sens Environ. 2015;170:121–32. https://doi.org/10.1016/j.rse.2015.09.004.
172.• White JC, Wulder MA, Hermosilla T, Coops NC, Hobart GW. A nationwide annual characterization of 25 years of forest disturbance and recovery for Canada using Landsat time series. Remote Sens Environ. 2017;194:303–21. https://doi.org/10.1016/j.rse.2017.03.035 **National-scale analysis of fire disturbances based on multitemporal RS images**.
173. Griffiths P, Kuemmerle T, Baumann M, Radeloff VC, Abrudan IV, Lieskovsky J, et al. Forest disturbances, forest recovery, and changes in forest types across the Carpathian ecoregion from 1985 to 2010 based on Landsat image composites. Remote Sens Environ. 2014;151:72–88. https://doi.org/10.1016/j.rse.2013.04.022.
174. Frazier RJ, Coops NC, Wulder MA, Hermosilla T, White JC. Analyzing spatial and temporal variability in short-term rates of post-fire vegetation return from Landsat time series. Remote Sens Environ. 2018;205:32–45. https://doi.org/10.1016/j.rse.2017.11.007.
175. Kennedy RE, Yang Z, Gorelick N, Braaten J, Cavalcante L, Cohen WB, et al. Implementation of the LandTrendr Algorithm on Google Earth Engine. Remote Sens. 2018;10(5):691. https://doi.org/10.3390/rs10050691.
176. Hughes MJ, Kaylor SD, Hayes DJ. Patch-based forest change detection from Landsat time series. Forests. 2017;8(5):166. https://doi.org/10.3390/f8050166.
177. Frazier RJ, Coops NC, Wulder MA. Boreal shield forest disturbance and recovery trends using Landsat time series. Remote Sens Environ. 2015;170:317–27. https://doi.org/10.1016/j.rse.2015.09.015.
178. Morresi D, Vitali A, Urbinati C, Garbarino M. Forest spectral recovery and regeneration dynamics in stand-replacing wildfires of Central Apennines derived from Landsat time series. Remote Sens. 2019;11(3):308. https://doi.org/10.3390/rs11030308.
179. Storey EA, Stow DA, O'Leary JF. Assessing postfire recovery of chamise chaparral using multi-temporal spectral vegetation index trajectories derived from Landsat imagery. Remote Sens Environ. 2016;183:53–64. https://doi.org/10.1016/j.rse.2016.05.018.

180. Hermosilla T, Wulder MA, White JC, Coops NC, Hobart GW, Campbell LB. Mass data processing of time series Landsat imagery: pixels to data products for forest monitoring. International Journal of Digital Earth. 2016;9(11):1035–54. https://doi.org/10.1080/17538947.2016.1187673.
181. Massetti A, Rüdiger C, Yebra M, Hilton J. The vegetation structure perpendicular index (VSPI): a forest condition index for wildfire predictions. RSE. 2019;224:167–81. https://doi.org/10.1016/j.rse.2019.02.004.
182. Hislop S, Jones S, Soto-Berelov M, Skidmore A, Haywood A, Nguyen TH. Using Landsat spectral indices in time-aeries to assess wildfire disturbance and recovery. Remote Sens. 2018;10(3):460. https://doi.org/10.3390/rs10030460.
183. Ryu JH, Han KS, Hong S, Park NW, Lee YW, Cho J. Satellite-based evaluation of the post-fire recovery process from the worst forest fire case in South Korea. Remote Sens. 2018;10(6):918. https://doi.org/10.3390/rs10060918.
184. Joao T, Joao G, Bruno M, Joao H. Indicator-based assessment of post-fire recovery dynamics using satellite NDVI time-series. Ecol Indic. 2018;89:199–212. https://doi.org/10.1016/j.ecolind.2018.02.008.
185. Matasci G, Hermosilla T, Wulder MA, White JC, Coops NC, Hobart GW, et al. Three decades of forest structural dynamics over Canada's forested ecosystems using Landsat time-series and Lidar plots. Remote Sens Environ. 2018;216:697–714. https://doi.org/10.1016/j.rse.2018.07.024.
186. Chen W, Jiang HZ, Moriya K, Sakai T, Cao CX. Monitoring of post-fire forest regeneration under different restoration treatments based on ALOS/PALSAR data. New For. 2018;49(1):105–21. https://doi.org/10.1007/s11056-017-9608-2.
187.• Polychronaki A, Gitas IZ, Minchella A. Monitoring post-fire vegetation recovery in the Mediterranean using SPOT and ERS imagery. Int J Wildland Fire. 2014;23(5):631–42. https://doi.org/10.1071/wf12058 **Analysis of post-fire vegetation trends from satellite imagery.**